

See discussions, stats, and author profiles for this publication at: <https://www.researchgate.net/publication/266440202>

# CO<sub>2</sub> Sorption Enhanced Steam Reforming of Ethanol

## ARTICLE

---

READS

37

## 6 AUTHORS, INCLUDING:



[Tiejun Zhao](#)

Chinese Academy of Sciences

34 PUBLICATIONS 400 CITATIONS

[SEE PROFILE](#)



[Edd A. Blekkan](#)

Norwegian University of Science and Tech...

85 PUBLICATIONS 2,130 CITATIONS

[SEE PROFILE](#)



[De Chen](#)

Norwegian University of Science and Tech...

235 PUBLICATIONS 4,782 CITATIONS

[SEE PROFILE](#)

# Approaching Sustainable H<sub>2</sub> Production: Sorption Enhanced Steam Reforming of Ethanol<sup>†</sup>

Li He, Helene Berntsen, and De Chen\*

Department of Chemical Engineering, Norwegian University of Science and Technology, Sem Sælands vei 4, Trondheim, NO-7491, Norway

Received: June 30, 2009; Revised Manuscript Received: September 24, 2009

Sorption enhanced steam reforming of ethanol (SESRE), featured by yielding high purity of H<sub>2</sub> from one single reaction unit, is a new reaction process with a great potential for realizing sustainable H<sub>2</sub> production. The potential of such process with a CaO-based acceptor has been assessed by thermodynamic analysis and experimental demonstration. As predicted, ethanol can be reformed at relatively low temperatures (500–600 °C), still yielding high-quality H<sub>2</sub>. Another major advantage of coupling CO<sub>2</sub> capture to the reforming process is predicted to be low risk in carbon formation. The SESRE reaction was carried out over a mixture of hydrotalcite-like material derived Co–Ni catalysts (Co–Ni/HTIs) and calcined dolomite with a steam to carbon (S/C) ratio of 3 and temperatures ranging from 500 to 650 °C. The chosen reaction system was able to yield H<sub>2</sub> with purity fairly close to the theoretical prediction. Particularly, the best result was obtained over 40Ni and 20Co-20Ni/HTIs at 550 °C, where the product gas had composition of more than 99 mol % H<sub>2</sub>, ca. 0.4 mol % CH<sub>4</sub>, 0.1 mol % CO, and 0.2 mol % CO<sub>2</sub>. Special emphasis was put on the effect of steam on the stability of the CO<sub>2</sub> acceptor during the SESRE reaction. Hydration of CaO in the acceptor did not cause appreciable induction period, even at the low operating temperatures. However, different from a test under dry atmosphere (CO<sub>2</sub>/argon), the acceptor showed rapid deactivation in a multicycle operation of SESRE. A similar deactivation trend was given by a comparative test in a steam/CO<sub>2</sub>/Ar atmosphere.

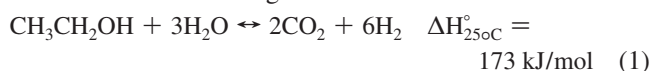
## I. Introduction

The demand of H<sub>2</sub> in future has been forecasted to increase not only for conventional industrial use but also for clean energy generation, particularly in fuel cell application. Today, 95% H<sub>2</sub> in the current industrial production comes from the steam reforming of natural gas. The depletion of global fossil fuel resources, growing environmental impact and energy security concerns urge new alternatives for H<sub>2</sub> production. In this context, conversion of cheap and available biomass or biomass-derived chemicals for H<sub>2</sub> production is considered to be a promising approach to quench the need of H<sub>2</sub> and, meanwhile, to realize sustainable development. In addition to the common features of biobased fuels, such as CO<sub>2</sub> neutrality and renewability, ethanol can be produced from a diversity of low-valued feedstocks, including corn, wood waste, municipal solid waste, grasses-offering and so on.<sup>1</sup> Besides, direct conversion of ethanol diluted with water can avoid energy demanding step for ethanol purification. Integrating ethanol production with hydrogen production might have great economic potential in utilization of biomass for renewable energy production.

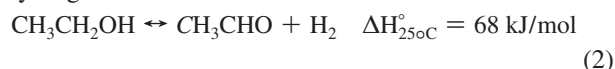
Ethanol-fueled processes for H<sub>2</sub> production has been explored mainly by thermochemical means, typically steam reforming of ethanol.<sup>2,3</sup> The ideal complete steam reforming of ethanol is presented in eq 1. It is hardly accomplished in practice due to the reaction reversibility, coke formation, and undesired reaction paths. Indeed, ethanol reforming can have rather complex product distribution. The reactions represented in eqs 2–8 have been observed and play important roles in determining product species.<sup>4,5</sup> As a result, the product gas out of the reformat has

limited H<sub>2</sub> purity and high carbon oxide contents. This can be improved by using membrane or double-layered catalytic reactor.<sup>6,7</sup> However, in addition to the common problems in steam reforming processes, the operation of those techniques is challenged by their own practical issues, for example, limited separation efficiency of membrane or difficult control of operation. As a result, the purity of hydrogen produced from such processes is sacrificed.

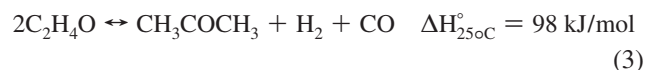
Ethanol steam reforming



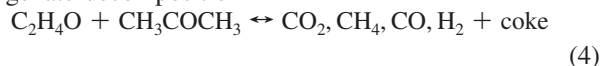
Dehydrogenation of ethanol



Aldol condensation



Oxygenate decomposition



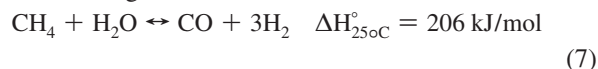
Dehydration of ethanol



Ethylene reforming



Steam reforming of methane



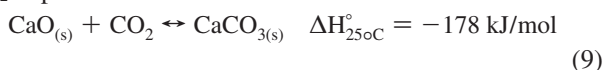
<sup>†</sup> Part of the special issue “Green Chemistry in Energy Production Symposium”.

\* To whom correspondence should be addressed. Tel: +47 73593149. Fax: +47 73595047. E-mail: chen@nt.ntnu.no.

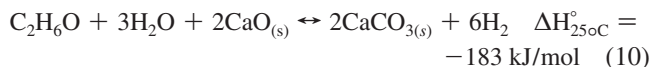
Water shift reaction



CO<sub>2</sub> capture



Overall SESRE



On the other hand, a new reaction process has been proposed to improve H<sub>2</sub> production by steam reforming. The concept of sorption-enhanced steam reforming (SESR) is based on Le Chatelier's principle in which the reaction equilibrium will be shifted to favor increase of the reactant conversion upon in situ removal of any of the products. Accordingly, if CO<sub>2</sub> generated from the steam reforming process is separated from gas phase by using solid acceptor such as CaO, H<sub>2</sub> production can be enhanced toward completion. The CO<sub>2</sub> capture and overall SESRE reaction are illustrated in eqs 9 and 10, respectively.

The appealing features of sorption-enhanced steam reforming of methane (SESRM) for H<sub>2</sub> production has been demonstrated in the recent studies.<sup>6,8</sup> Relative to 72 mol % H<sub>2</sub> (dry basis) in the product gas of single SMR reactor, a much high H<sub>2</sub> content at 94% was obtained with the addition of CaO as CO<sub>2</sub> acceptor at operating conditions of 750 °C, a steam to carbon ratio (S/C) = 3 and 1 atm.<sup>9</sup> With optimization of the SESR operating conditions, H<sub>2</sub> purity can be even further improved. For example, the H<sub>2</sub> concentration reached 98–99 mol % at 600 °C and 1 atm with dolomite as CO<sub>2</sub> acceptor.<sup>10</sup> According to simulation results, a fuel-cell grade H<sub>2</sub> can be directly produced with very high CH<sub>4</sub> to H<sub>2</sub> conversion in a SESR operation unit with hydrotalcite as CO<sub>2</sub> sorbent.<sup>11</sup> Besides high H<sub>2</sub> production efficiency, the other advantages of SESR are expected, including less coke formation, easy CO<sub>2</sub> sequestration or recovery, possible reduced surface area of the heat transfer utilities.<sup>12</sup>

To date, most of SESR study has been focused on the use of CH<sub>4</sub> as feedstock, while little has been done on ethanol. The distinct chemical properties of ethanol and the complicated reaction mechanism of ethanol reforming require thorough investigation on sorption-enhanced steam reforming of ethanol (SESRE) for application of H<sub>2</sub> production. Lysikov et al. have compared various hydrocarbon fuels for H<sub>2</sub> production via SESR over an admixture of a CaCO<sub>3</sub>-calcined acceptor and commercial Ni catalyst.<sup>13</sup> Ethanol exhibited advantage over the other studied fuels by yielding high quality H<sub>2</sub>. Iwasaki et al. have conducted SESRE experimental study with 1 wt % Rh/CeO<sub>2</sub> catalyst and Li<sub>4</sub>SiO<sub>4</sub> as sorbent and have demonstrated that the highest H<sub>2</sub> purity was 96% at 550 °C.<sup>14</sup> Essaki et al. have claimed that the concentration of H<sub>2</sub> above 99%, together with CO below 0.12%, was achieved by SESRE with commercial 58 wt % Ni/Al<sub>2</sub>O<sub>3</sub> catalyst and Li<sub>4</sub>SiO<sub>4</sub> as sorbent, operated at 577–627 °C, 1 atm, and S/C = 3.<sup>15</sup>

Although such reported results are encouraging, there are still a lot of challenges to make the new process more economically feasible. Selection of CO<sub>2</sub> acceptor has great impact on SESRE process. CaO-based materials have been suggested as suitable candidates with favorable equilibrium partial pressure of CO<sub>2</sub> and kinetics for CO<sub>2</sub> removal.<sup>16</sup> Dolomite is a relatively cheap and naturally occurring material, which forms a mixture of CaO-MgO upon calcination.<sup>17,18</sup> MgO is inert to CO<sub>2</sub> at the temperature of interest for SESRE, typically at 450–750 °C. CaO incorporated in a matrix of MgO is able to absorb CO<sub>2</sub> with competitive cyclic stability among CaO-based acceptors.<sup>17</sup>

SESRE is a hybrid process of CO<sub>2</sub> capture and catalytic reforming of ethanol, where the catalyst plays an important role in ethanol conversion. Catalysts used in SESRE processes are often Ni-based commercial catalysts. Even though the Ni-based catalysts work well for ethanol reforming by promoting C–C cleavage, they are not optimized for SESRE. To enhance hydrogen production with shifted equilibrium by removing CO<sub>2</sub>, the catalyst is required to have high activity at the low temperatures where CO<sub>2</sub> removal is favored. This might be realized by altering the property of Ni-based catalyst with addition of Co.<sup>19</sup> The Co–Ni catalysts derived from hydrotalcite-like materials (HTls) have exhibited high activity and good stability in the test on stream with the steam reforming of ethanol. Besides the expected synergic effect on H<sub>2</sub> production, both Ni and Co can function as oxygen carrier to facilitate chemical looping and autothermal reforming. Thereby, investigation on Co–Ni catalyst might offer opportunity to cut down energy cost in H<sub>2</sub> production by integrating the SESRE process with chemical looping or autothermal reforming. In addition, high metal loading of the Co–Ni/HTls catalysts was designed in the catalyst development, intending to reduce the size of the reactor. It is based on the consideration that reactor size can be an issue in the application of SESRE since CO<sub>2</sub> acceptor needs to be installed together with the catalyst, requiring more space of the reactor than that for a typical steam reforming reaction.

The appealing properties of the Co–Ni/HTls catalysts have made themselves competitive candidates as catalysts for the SESRE reaction. In this work, the Co–Ni/HTls catalysts, together with calcined dolomite as CO<sub>2</sub> acceptor, were installed in a fixed bed reactor to carry out the SESRE reaction. Before the experimental demonstration, the SESRE reaction process was analyzed from thermodynamic approach, by which a possible operating window was suggested for enhancing H<sub>2</sub> productivity.

## II. Experimental Methods

**1. Catalyst and Acceptor.** A series of hydrotalcite-like (HTls) derived Co–Ni catalysts was prepared by coprecipitation. The total metal loading was fixed at 40 wt % and the Co–Ni composition varied from 40:0 to 30:10, 20:20, 10:30, and 0:40. The detailed preparation procedure and catalyst test on stream are described elsewhere.<sup>19</sup> The naturally occurred dolomite (Arctic dolomite) was purchased from Franzefoss Miljøkalk A/S. The chemical composition of CaMg(CO<sub>3</sub>)<sub>2</sub> is documented as ca. 98.5% and no sulfur indicated by the X-ray fluorescence analysis. In this work, all of the dolomite samples were calcined at 800 °C in air flow for 4 h before application.

**2. Experimental Demonstration of SESRE.** A typical procedure is described as the following. A mixture of Co–Ni/HTls catalyst (2 g) and calcined dolomite (10 g) was placed in a steel reactor (i.d. 16 mm). Prior to the SESR procedure, the calcined catalyst was reduced at 670 °C (heating rate 10 °C/min) for 10 h in a mixed flow of H<sub>2</sub> (50 mL/min) and Ar (50 mL/min). The gases were delivered by Bronkhorst gas mass flow controllers (MFC). The SESRE operation procedure was divided into two sessions, the SESRE and acceptor regeneration. The first session for the steam reforming and CO<sub>2</sub> capture reaction was operated typically as the following description. A liquid fuel–water mixture at a given steam to carbon ratio was fed by a Bronkhorst liquid flow controller (LMFC), swept by Ar flow of 25 mL/min, evaporated in a vaporizer and then directed into the reactor. The SESRE reaction was carried out in a temperature range of 500–650 °C, with a liquid flow of ca. 5.7 g/h and N<sub>2</sub> flow of 21 mL/min as an internal standard.

The reactor effluent was directed into a water-cooling condenser, followed by a membrane gas drier. Most of high boiling point products were collected in the condenser and regularly drained out. The examination of liquid effluent was performed with  $^1\text{H}$  nuclear magnetic resonance (NMR) spectroscopy according to the description elsewhere.<sup>19</sup> The exiting gas flow was analyzed with an online Agilent M3000 Miro GC, equipped with a Plot U and Molsieve molecular sieve column. The SESRE session continued until the breakthrough of  $\text{CO}_2$  content occurred, indicated by its fast increase. In the following session, the acceptor was thermally regenerated at  $770^\circ\text{C}$  for 0.5 h with a ramp rate of  $2^\circ\text{C}/\text{min}$ . Ar flow of 50 mL/min was used to sweep the released  $\text{CO}_2$  and, at the same time,  $\text{H}_2$  flow of 10 mL/min was fed to keep the Ni and Co in metal state. Afterward, the temperature of the reactor was regulated for a new SESRE session. The SESRE and regeneration session repeated cyclically. Ar flow of 75 mL/min was used to flush the reaction system for ca. 1 h before a new session started. In some cases, the SESRE session was extended to carry out a conventional steam reforming reaction after the breakthrough of  $\text{CO}_2$  content occurred. It should be mentioned that hydrogen production from bioethanol is considered as a  $\text{CO}_2$  neutral process, the  $\text{CO}_2$  sequestration is not necessary for this process.

The following equation was used to estimate the ultimate capacity of the dolomite in the cyclic operation:

$$N_{\text{CO}_2} = \int_0^{t_1} (F_{\text{CO}_2, \text{SR}} - F_{\text{CO}_2}) dt \quad (11)$$

Here,  $F_{\text{CO}_2, \text{SR}}$  represents the average value of  $\text{CO}_2$  flow rate during the course of the conventional steam reforming reaction;  $F_{\text{CO}_2}$  represents the  $\text{CO}_2$  flow rate at time  $t$ ;  $t_1$  represents the time point where the  $\text{CO}_2$  content in the gas effluent did not increase any more after the breakthrough started.

### 3. The Tapered Element Oscillating Microbalance (TEOM).

The cyclic stability of dolomite in steam-containing atmosphere was tested by using the TEOM. The measurement of the mass change in the sample bed is based on changes in the natural frequency of an oscillating quartz element containing the sample.<sup>20</sup> Ten milligrams of the sorbent was loaded on the tapered element and firmly packed to form the reaction bed. The sample was heated up to  $650^\circ\text{C}$  at a heating rate of  $10^\circ\text{C}/\text{min}$  and refreshed with Ar for 1 h. The weight of the sample was allowed to equilibrate at  $595^\circ\text{C}$  before the reactant mixture was fed into the tapered element to trigger the carbonation reaction. The reactant gas composition was chosen as 50% steam/10%  $\text{CO}_2/\text{Ar}$ , approximating the SESRE conditions. After saturation of the acceptor, the feed gas was switched to Ar and the sample was regenerated at  $700^\circ\text{C}$ . The time for carbonation and regeneration was 25 and 30 min.

**4. Thermal Gravimetric Analysis (TGA).** The major advantage of TGA is easy operation and experimental simplicity; a temperature programmed run can gather data sets for capture/regeneration capacity and kinetics. However, due to the instrument limitation, it is difficult to use TGA to conduct a high temperature measurement with gas flow containing steam at a well-defined partial pressure. On the other hand, the TEOM can be used to evaluate the effect of steam addition on the properties of  $\text{CO}_2$  acceptor.<sup>21</sup> But the difficult operation and low availability of the TEOM make it inconvenient choice in some cases. Therefore, in this paper, the cyclic stability of dolomite in steam-containing atmosphere was tested with the TEOM, while the test under dry conditions was performed by using a Netzsch STA 449 instrument, a thermal gravimetric analyzer. The

temperature program and atmosphere with TGA were chosen as the same as that in the TEOM experiment, except that a flow of 10%  $\text{CO}_2/\text{Ar}$  was fed in carbonation step.

Temperature-programmed oxidation (TPO) was also carried out on the same instrument. About 10 mg of the solid mixture spent from the SESRE experiment was weighed and placed in a sample holder. The sample was heated from room temperature to  $200^\circ\text{C}$  at  $10^\circ\text{C}/\text{min}$  in a flow of 50% air/Ar. The temperature was kept at  $200^\circ\text{C}$  for 1 h, before switching to a flow of 40%  $\text{CO}_2/\text{Ar}$  and heating the sample at  $10^\circ\text{C}/\text{min}$  to  $450^\circ\text{C}$ . After the temperature had been kept at  $450^\circ\text{C}$  for 4 h, the TPO was performed with a ramp of  $2^\circ\text{C}/\text{min}$  in a flow of 40% air/40%  $\text{CO}_2/\text{Ar}$ . The measurement ended when the temperature reached  $800^\circ\text{C}$ .

## III. Results and Discussion

**1. Thermodynamic Equilibrium Analysis.** As mention before, steam reforming of ethanol is a complex process. The product composition is governed by the global thermodynamic equilibrium of all possible species involved in the reactions represented in eqs 1–7. Knowledge of this equilibrium is essential for discussing experimental results. Thereby, before the experimental demonstration, thermodynamic analysis has been conducted. The calculation was carried out by programming codes in MATLAB 6.1, combined with thermodynamic properties in FactSage 5.1. The equilibrium compositions were calculated by minimizing the Gibb's free energy without specification of the possible reactions taking place. This requires identification of the possible products. According to the reported results for the equilibrium prediction of C–H–O system under gasification conditions, the present species at concentrations greater than  $10^{-4}$  mol % are only  $\text{H}_2$ , CO,  $\text{CO}_2$ ,  $\text{CH}_4$ ,  $\text{H}_2\text{O}$ , and solid carbon (graphite) as products.<sup>22</sup> In several thermodynamic studies on simulation of the steam reforming reaction of oxygenated hydrocarbons, the compounds, such as ethane, ethylene, acetylene, or various organic oxygenates, have been included to the product pool.<sup>23–26</sup> However, the predicted results reached an agreement that only  $\text{H}_2$ , CO,  $\text{CO}_2$ ,  $\text{CH}_4$ ,  $\text{H}_2\text{O}$ , and solid carbon in the equilibrium stream could have concentrations great enough to be considered as the products in the practice of modeling. On the basis of the above results, we argue that it is reasonable to predict the equilibrium state of the product stream from steam reforming of ethanol based on the product pool including  $\text{H}_2$ , CO,  $\text{CO}_2$ ,  $\text{CH}_4$ ,  $\text{H}_2\text{O}$ , and solid carbon. The same operating conditions were used for the SESRE reaction process, except that CaO,  $\text{Ca}(\text{OH})_2$ , and  $\text{CaCO}_3$  were added to the system. CaO was in the stoichiometric ratio to carbon atoms (or  $\text{CaO}/\text{ethanol} = 2/1$  for the initial condition of the simulation) in the system. The calculation was conducted in the range defined by steam-to-fuel ratio = 0.5:9, reaction temperature =  $450\text{--}750^\circ\text{C}$ , and pressure = 1–20 bar. Product mole fractions in Figures 1 and 2 are given on a dry basis. Namely, the total number of moles is determined only by  $\text{H}_2$ ,  $\text{CH}_4$ , CO,  $\text{CO}_2$ , and carbon.

The addition of steam is expected to help  $\text{H}_2$  production and coke reduction. Figure 1 shows the equilibrium composition as a function of temperature and steam-to-fuel ratio by steam reforming of ethanol with or without the presence of CaO. A similarity is observed between both the cases of ethanol reforming. When steam-to-fuel ratio is below the stoichiometric ratio of 3 defined in reaction 1, ethanol reforming in both the processes is steam-limited.  $\text{H}_2$  production and carbon formation have strong dependence on the amount of steam, in particular, without the presence of CaO.  $\text{H}_2$  molar fraction increases rapidly



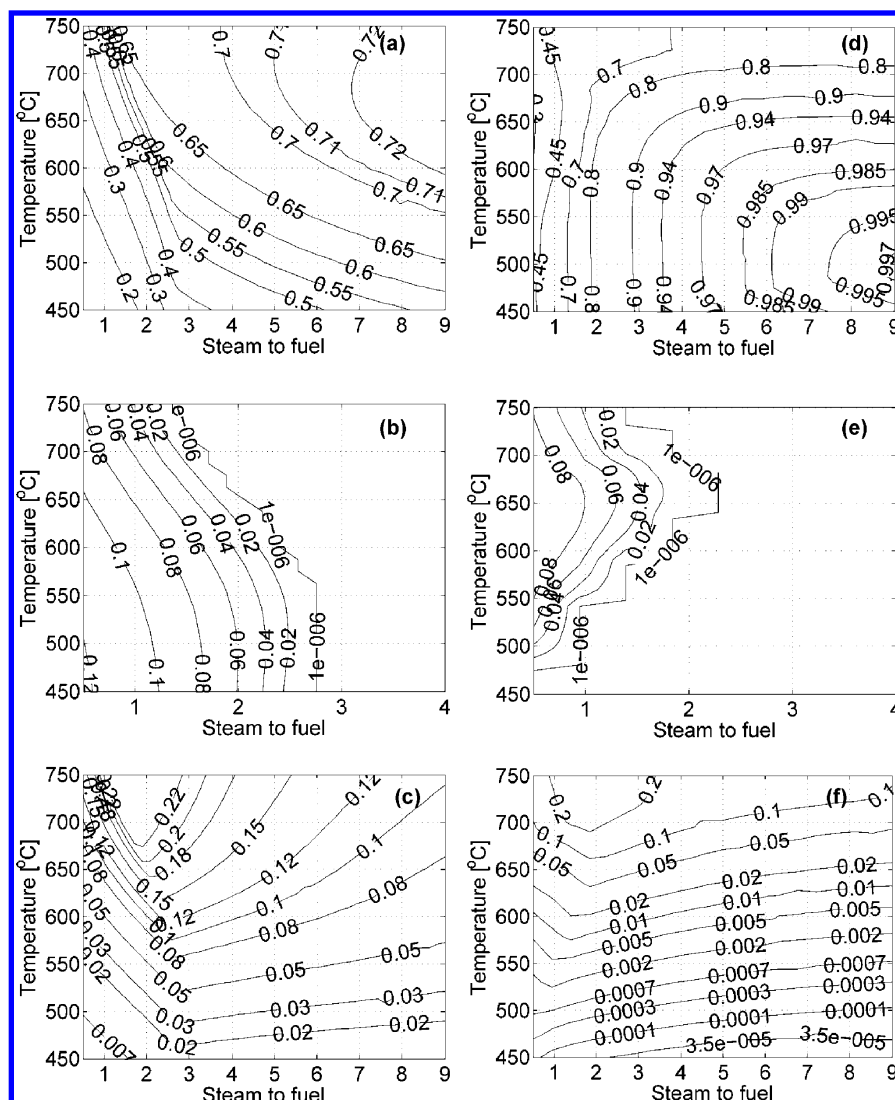


**Figure 1.** Effects of temperature and steam-to-fuel ratio on the dry basis mole fractions of H<sub>2</sub> (a,d), carbon (b,e), and CO (c,f). The plots (a–c) are for steam reforming of ethanol and (d–f) for sorption-enhanced steam reforming of ethanol under atmospheric pressure.

as the steam-to-fuel ratio increases. Carbon formation is largely reduced as the steam-to-fuel ratio is elevated from 0.5 to 2. On the other hand, when steam is used in excess the steam-to-fuel ratio no longer has a strong effect on the ethanol reforming reactions while temperature becomes important parameter to the H<sub>2</sub> production.

Nevertheless, the advantage of SESRE can be highlighted by its distinct difference from the ethanol steam of ethanol. First, as shown in Figure 1a,d, much higher H<sub>2</sub> molar fraction in SESRE is expected than that from the steam reforming of ethanol at the corresponding conditions. It is known that the economy of H<sub>2</sub> production via the conventional steam reforming is considerably compromised by cost for generating a large amount of excess steam, necessary for improving H<sub>2</sub> content in the product gas. In contrast, when coupled with CO<sub>2</sub> removal, the steam reforming reaction process is able to yield high concentration of H<sub>2</sub> with relatively low steam-to-fuel ratio. Reduced steam consumption might lead to superior thermal efficiency for H<sub>2</sub> production. What's more, Figure 1d indicates that H<sub>2</sub> production by SESRE operated in the low temperature regime is much better enhanced than in the high temperature regime. It can be attributed to the exothermic effect of CO<sub>2</sub> capture on the overall reaction of SESRE. The simulation results presented in Figure 1d further suggests that it is possible to

carry out low-temperature steam reforming and at the same time obtain high concentration of H<sub>2</sub> in the product gas. More benefits of SESRE can be seen by comparing the carbon contents in the systems shown in Figure 2b,d. To avoid carbon formation, the steam-to-fuel ratio of above ca. 3 is thermodynamically necessary in the conventional steam reforming reaction process. The limit of steam-to-fuel ratio for carbon free operation is shifted down to ca. 2 in the presence of CaO. The addition of CaO is expected to reduce solid carbon content, implying that the SESRE reaction system has low risk of solid carbon formation.

The effect of temperature and pressure on H<sub>2</sub> production is examined at the steam-to-fuel ratio of 6. The simulation results for H<sub>2</sub> content are presented in Figure 2a,c, respectively, for with and without CaO addition. It is seen that an increase of pressure has an adverse effect on the H<sub>2</sub> output in both of cases. However, compared to the severe reduction of the H<sub>2</sub> content from the process without the addition of CaO, a moderate decline is observed on the H<sub>2</sub> content with the addition of CaO. The less dependence of the H<sub>2</sub> content on operating pressure further verifies the attractiveness of SESRE since high pressure is preferred in industrial operation for the overall process economy.

One of arguments on application of CaO-based material as CO<sub>2</sub> acceptor in steam-rich atmosphere is the affinity of CaO

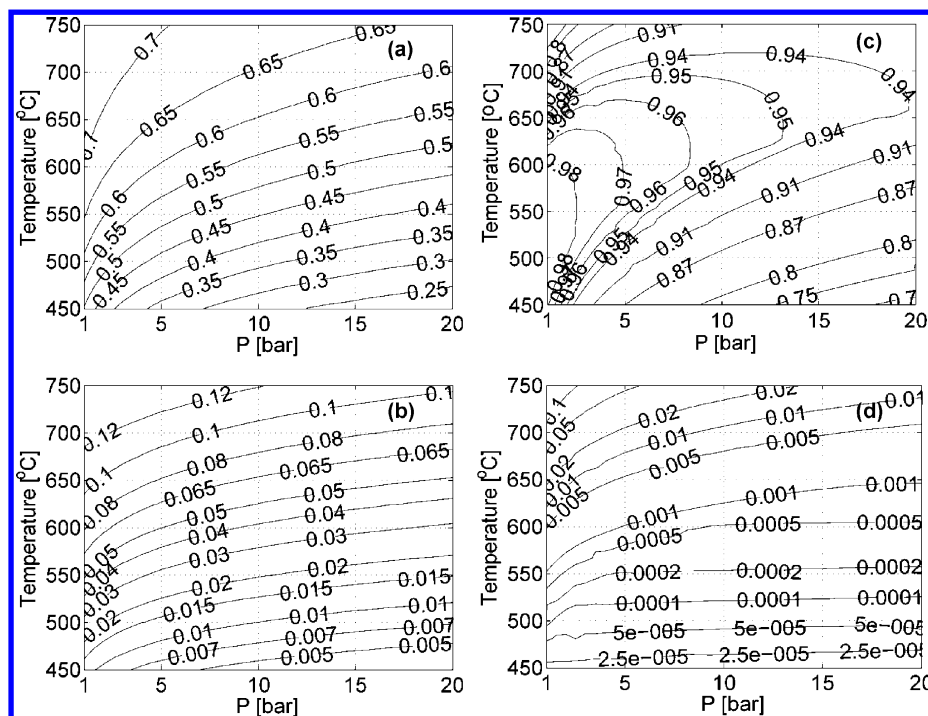


**Figure 2.** Effects of temperature and pressure on the dry basis mole fractions of  $H_2$  (a,c) and  $CO$  (b,d). The plots (a,b) are for steam reforming of ethanol and (c,d) for sorption enhanced steam reforming of ethanol with a steam-to-fuel ratio of 6.

to water. Low-temperature operation of SESRE is beneficial to  $H_2$  production since  $CO_2$  capture is thermodynamically favored and evident enhancement in the  $H_2$  output is expected. However, there is a low limit on the temperature for operating SESRE in order to prevent preferential adsorption of steam on  $CaO$ . As shown in Figure 1d, the  $H_2$  content decreases with a decrease in the reaction temperature when it is less than  $500\text{ }^{\circ}C$ . The observed trend is in accordance with that lowering the temperature increases the affinity of  $CaO$  toward steam and less  $CaO$  is available to  $CO_2$ . As a result, the inferior enhancement in  $H_2$  production is expected at temperatures lower than  $500\text{ }^{\circ}C$ . It is worthy mentioning that the influence of  $CaO$  hydration becomes more evident at high pressures. Even though high pressure operation improves  $CO_2$  capture, it also increases the affinity of  $CaO$  toward steam. As shown in Figure 2c, the highest  $H_2$  content is predicted at ca.  $650\text{ }^{\circ}C$  when the SESRE is operated at a pressure of 15 bar while the maximum is at ca.  $500\text{ }^{\circ}C$  in atmosphere-pressure operation.

Thermodynamic analysis can be used as a valuable tool for optimization of operating parameters. For example,  $CO$  content is an important issue in the application of  $H_2$  for energy generation. The change of  $CO$  content with temperature and steam-to-fuel ratio in the reforming process is shown in Figure 1c,f and with temperature and pressure in Figure 2b,d. It is seen that the SESRE reaction process is able to yield much lower  $CO$  content than the conventional steam reforming of ethanol at the corresponding conditions. With an objective of minimization of  $CO$  content, low temperature operation of SESRE might be desirable. In addition, increasing operating pressure might be helpful to reduce  $CO$  content. On the other hand, little variation of  $CO$  content is expected as the steam-to-fuel ratio increases since it is not sensitive to the steam-to-fuel ratio.

**2. Experimental Demonstration.** The thermodynamic analysis provides a helpful picture for optimization of  $H_2$  production, oriented with end-client applications. However, the application of SESRE is complicated by the coupling effect of catalytic and  $CO_2$  removal reactions. The gas effluent composition out

of a SESRE reactor is not only determined by typical operating parameters for catalytic reactions, such as the chosen catalyst, gas residence time, temperature, pressure, steam-to-carbon, but also by the chosen acceptor, ratio of catalyst to acceptor, mixing between the catalyst and acceptor, and chemical or physical interaction between the catalyst and acceptor. Catalytic steam reforming is regarded as surface-gas reaction, whose intrinsic kinetics is governed by the catalyst surface properties, whereas the  $CO_2$  removal is a typical solid–gas reaction, where the solid-state diffusion of  $CO_2$  in the bulk material of the acceptor is rate-limiting step. The two parallel reaction mechanisms lead to different behaviors to changes in operating conditions.

The experiments with a mixture of  $Co-Ni/HTIs$  catalysts and calcined dolomite were carried out in a fixed-bed over a temperature range from  $500$  to  $650\text{ }^{\circ}C$ , at 1 atm and steam-to-fuel of 6 (or  $S/C = 3$ ). The operating window of the temperature is chosen for maintaining both suitable catalytic activity and efficient  $CO_2$  removal. According to the thermodynamic prediction, the steam-to-fuel of 6 is sufficient to prevent coke formation, and further increasing the steam-to-fuel ratio will not lead to substantial improvement in  $H_2$  production.

Typically, the evolution of the gas effluent compositions in the SESRE reaction process takes three stages: prebreakthrough, breakthrough, and postbreakthrough. For example, Figure 3 shows that the product  $H_2$ ,  $CO$ ,  $CO_2$ , and  $CH_4$  concentrations as a function of time from a test at  $550\text{ }^{\circ}C$  with  $40Ni/HTIs$ . During the prebreakthrough phase, the calcined dolomite was active to capture  $CO_2$ , and thereby the  $CO_2$  concentration was low. At the same time, the ethanol reforming reactions were driven toward completion by the  $CO_2$  removal. The byproduct of  $CH_4$  and  $CO$  were minimized and  $H_2$  production was enhanced to high efficiency. Because of its nature, the SESRE reaction has strong dependence on the  $CO_2$  removal. It is well-known that the  $CaO-CO_2$  reaction has a fast reaction regime, followed by a fairly slow reaction regime controlled by  $CO_2$  diffusion through the layer of solid  $CaCO_3$  product formed on the  $CaO$ .<sup>27–30</sup> As the SESRE reaction proceeded, the  $CaO-CO_2$

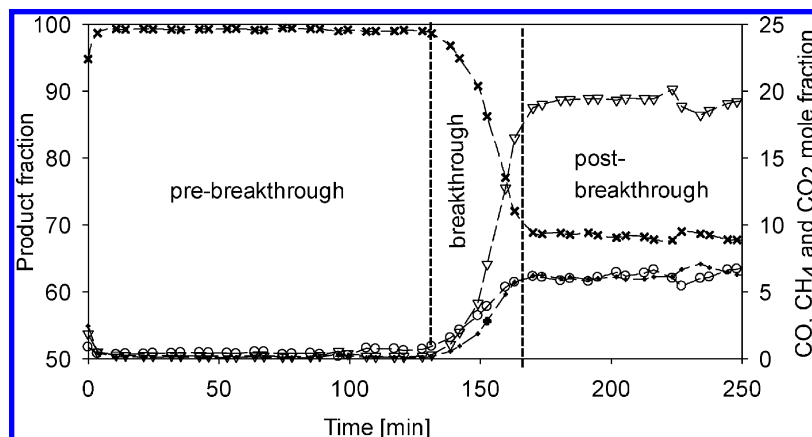


**Figure 3.** Effluent gas composition evolution in the reactions of the sorption enhanced steam reforming of ethanol. The conditions were at a temperature of 550 °C, a pressure of 1 atm, and a steam-to-fuel ratio of 6. A mixture of dolomite (10 g) and 40Ni/HTIs (2 g) was used.

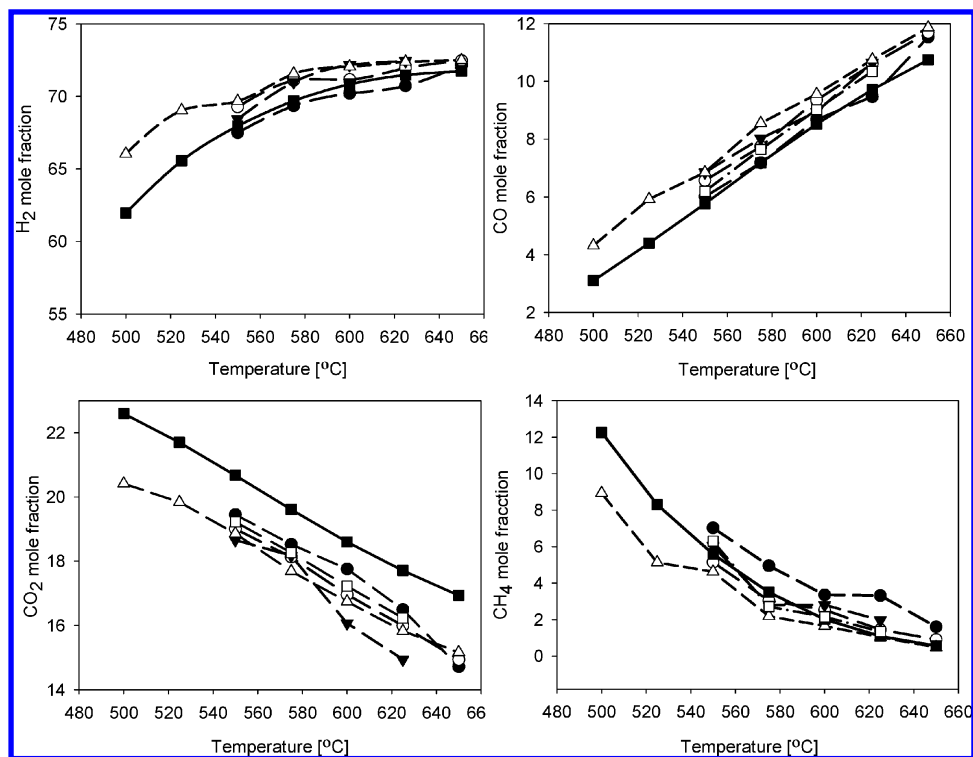


**Figure 4.** Effluent gas compositions obtained during the stabilized postbreakthrough stage. The conditions are the following: a pressure of 1 atm, a steam-to-fuel ratio of 6, and a mixture of dolomite (10 g) and Co–Ni/HTIs (2 g). (■) Equilibrium; (□) 40Ni; (Δ) 40Co; (▼) 30Co–10Ni; (○) 20Co–20Ni; (●) 10Co–30Ni.

reaction of acceptor approached the second reaction regime. The breakthrough represented the transition of the CaO–CO<sub>2</sub> from the first to the second regime. As seen in Figure 3, during the stage of breakthrough, the CO<sub>2</sub> content increased rapidly. After the second regime was started, the very limited remaining CO<sub>2</sub> capture was negligible and had little influence on the steam reforming of ethanol.

**A. Postbreakthrough: Conventional Steam Reforming of Ethanol.** To better understand the coupling effect of catalytic and CO<sub>2</sub> removal reaction, discussion on the steam reforming reaction is given before we analyze the experimental results from the SESRE reaction. The results from the postbreakthrough stage, corresponding to the steam reforming reaction with negligible CO<sub>2</sub> removal, are assumingly representative to those from the conventional catalytic reactions. Figure 4 shows the effluent gas compositions obtained during the stabilized postbreakthrough stage with the different catalysts. The mole fractions of H<sub>2</sub> were near to the equilibrium value, indicating

that the steam reforming reaction of ethanol ran at its maximum efficiency and the activities of all the catalysts were sufficient. Some of the H<sub>2</sub> mole fractions were slightly over the equilibrium. It might be caused by the remaining low activity of the dolomite to CO<sub>2</sub> capture after the breakthrough of the CO<sub>2</sub> contents. A small amount of CO<sub>2</sub> removal in this stage can shift slightly the equilibrium.

The results from the previous study have discovered that the steam reforming of ethanol over the Co–Ni/HTIs catalysts occurred mainly through the formation of acetate by dehydrogenation of ethanol.<sup>19</sup> As reaction intermediate, acetate further decomposed to CH<sub>4</sub> and CO<sub>2</sub> via decarbonylation reaction.<sup>5</sup> The composition of produced mixture was further changed through the reactions, presented in eqs 7 and 8. CH<sub>4</sub> was reformed with steam to generate H<sub>2</sub> and CO and afterward CO further reacted to undergo the water shift reaction to produce CO<sub>2</sub>. Accordingly, CH<sub>4</sub> was consumed by the steam reforming of methane or generated by its reverse reaction, methanation of CO, depending

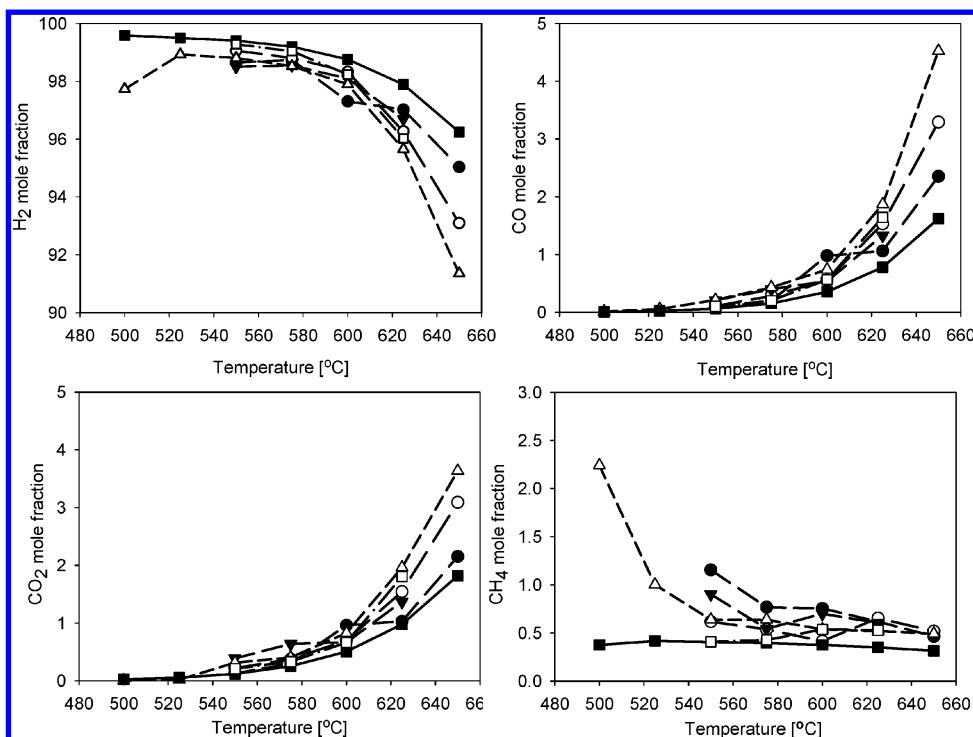


**Figure 5.** Effluent gas compositions obtained during the stabilized prebreakthrough stage. The conditions are the following: a pressure of 1 atm, a steam-to-fuel ratio of 6 and a mixture of dolomite (10 g) and Co–Ni/HTIs (2 g). (■) Equilibrium; (□) 40Ni; (Δ) 40Co; (▼) 30Co–10Ni; (○) 20Co–20Ni; (●) 10Co–30Ni.

on the reaction conditions. In the low temperature regime, the endothermic reaction of methanation was favored by thermodynamics and might make an important contribution to  $\text{CH}_4$  formation. This probably explains high  $\text{CH}_4$  content in the effluent gas at the low temperatures. On the other hand, low  $\text{CH}_4$  content was detected at the high temperatures. It might be rationalized by speculation that the steam reforming of  $\text{CH}_4$  was promoted to have strong influence on the product distribution. In Figure 4, the CO and  $\text{CO}_2$  contents were respectively plotted as a function of temperature. Compared to the equilibrium values, slightly high selectivity to CO and low to  $\text{CO}_2$  are generally observed over the studied temperature range. It means that operating conditions were not optimal for the water shift reaction along.

**B. Prebreakthrough.** Figure 5 shows the compositions of the effluent gas from the ethanol steam reforming over the various catalysts combined with in situ  $\text{CO}_2$  removal. The sorption enhancement is clearly illustrated by comparing the results during the pre- and postbreakthrough stages. In situ  $\text{CO}_2$  removal resulted in very high  $\text{H}_2$  concentrations in all cases of SESRE. For example, the  $\text{H}_2$  purity exceeded 98 mol % over all the catalysts at 550 and 575 °C. The best result was given with 40Ni and 40Co/HTIs at 550 °C. The  $\text{H}_2$  purity was higher than 99 mol % and the impurity content was ca. 0.4, 0.1, and 0.2 mol % for  $\text{CH}_4$ , CO, and  $\text{CO}_2$  respectively. The very low CO concentration might eliminate the requirement to a reactor for the water shift reaction, and the very high purity of  $\text{H}_2$  can relieve burden on the downstream purification step to a large extent. High-quality  $\text{H}_2$  from one compact reaction unit is particularly attractive to portable  $\text{H}_2$  production or on-site  $\text{H}_2$  production for fuel cell application. Furthermore, the examination on the liquid effluent revealed unconverted ethanol and byproduct acetaldehyde but at very low levels of concentration. This allows us to believe that the amounts of acetaldehyde and ethanol had little effect on the  $\text{H}_2$  yield and the gas product composition was essential in the current paper. It is worthy

noticing that in some cases of studied conditions, the  $\text{H}_2$  yield was fairly close to the stoichiometric limit, which means one ethanol molecule gives 6  $\text{H}_2$  molecules, or 0.26 g  $\text{H}_2$ /g ethanol. To maximize utilization of fed fuel has been considered as an important aspect in the conversion of biomass-derived chemicals to energy carrier since the biomass-derived chemicals per mass are usually more expensive than conventional fossil fuels. The very high  $\text{H}_2$  yield realized in the experiments demonstrated the merit of SESRE.

**Temperature Effect.** Temperature is an important reaction variable in the SESRE process. The selection of temperature involves a trade-off between thermodynamic and kinetic limitations, considering that the reactions represented by eqs 1–3, 5, and 7 are endothermic while the reactions in eqs 8–10 are exothermic.

The exothermic property of the overall SESRE reaction represented in eq 10 suggests that decreasing operating temperature favors the production of  $\text{H}_2$ . However, as shown in Figure 5, relatively large deviations of the experimental  $\text{H}_2$  contents from the corresponding equilibrium values were given in the low temperatures of 500 and 525 °C. This can be attributed to high concentrations of  $\text{CH}_4$ , which were presented as the major impurity in the gas product shown in Figure 5. A speculation is made to rationalize the observed results. As presented in eq 9, the carbonation and decarbonation are respectively involved as forward and backward reaction in  $\text{CO}_2$  capture. Even though lowering operating temperature favored  $\text{CO}_2$  removal thermodynamically, it decreased the rate of the carbonation reaction.<sup>28</sup> On the contrary, as discussed before the methanation reaction in the gas mixture of the SESRE reaction process was promoted evidently at such low temperatures. The slow  $\text{CO}_2$  removal did not efficiently suppress the methanation reaction, and consequently a high content of  $\text{CH}_4$  was obtained in the product gas.

At temperatures higher than 600 °C, the comparable low  $\text{H}_2$  concentration might be explained by the equilibrium and kinetics



factor. First, at elevated temperatures, the reaction equilibrium between the carbonation and decarbonation reaction limits the CO<sub>2</sub> removal, suggested by the relative high equilibrium CO<sub>2</sub> partial pressure. The discrepancies of the obtained CO<sub>2</sub> concentrations from the corresponding equilibrium values were larger than those at the temperatures below 600 °C. It was likely caused by the decreased efficiency of the CO<sub>2</sub> removal. Elevating the temperatures increased the rate of carbonation as well as decarbonation. But as the temperature was above 600 °C, the increase of the decarbonation rate was evident. As an overall result of the two opposite reactions, the CO<sub>2</sub> removal was suppressed, leading to the relative high partial pressure of CO<sub>2</sub> in the reaction gas. It further had impact on the completion of the water shift reaction. As shown in Figure 5, the relatively large discrepancies of the CO concentrations from their corresponding equilibrium values were also observed at the temperatures above 600 °C.

The H<sub>2</sub> concentration is presented as a volcano curve in Figure 5, indicating the existence of an optimum temperature for H<sub>2</sub> production. The maximum of H<sub>2</sub> concentration, more than 99%, was reached at 550 °C, where the equilibrium value was fairly closely approached. Such result tells that a good balance was established between thermodynamic and kinetic limitations for all the steam reforming, water shift, and CO<sub>2</sub> removal reactions in the chosen reaction system. As mentioned before, the H<sub>2</sub> production in the SESRE reaction process is boosted by the equilibrium-shift effect of CO<sub>2</sub> removal. The thermodynamic minimum of CO<sub>2</sub> partial pressure imposes limitation on the lowest CO<sub>2</sub> content in the gas effluent of SESRE. Thereby, the ultimate H<sub>2</sub> purity obtained in the experimental demonstration is defined by the CO<sub>2</sub> capture equilibrium.

**Catalyst Effect.** Figure 5 shows the effluent gas compositions over the Co–Ni/HTIs catalysts. Compared to the results from the conventional ethanol steam reforming reaction, the difference caused by the catalyst in use was not evident at the temperature of 575 °C. With the increase of temperature, much different performance was presented by the catalysts. Among all of the catalysts, the 10Co–30Ni/HTIs catalyst showed optimal selectivity to H<sub>2</sub> by yielding low CO and CO<sub>2</sub> content, suggesting a good activity to water shift reaction at the high temperature above 575 °C. Unlike the results from the conventional ethanol steam reforming,<sup>20</sup> the 40Co/HTIs catalyst presented inferior promotion to H<sub>2</sub> production through the SESRE reaction. However, at the low temperature of 550 °C, 40Co/HTIs catalyst exhibited good selectivity for the production of H<sub>2</sub>. Considering that a good selectivity to H<sub>2</sub> was also observed over the 40Co/HTIs catalyst in the conventional ethanol steam reforming,<sup>19</sup> the SESRE reaction temperature over the same catalyst was extended to 525 and 500 °C. As seen in Figure 5, at such low temperature the activity of the 40Co/HTIs catalyst was not efficient to suppress CH<sub>4</sub> formation, leading to relatively greater discrepancy of H<sub>2</sub> content in the product gas from the equilibrium.

**Induction Period.** Undesired interaction of the acceptor with the reactants or products in the steam reforming reaction may lead to reduction in CO<sub>2</sub> capture and fuel conversion efficiencies. As discussed above, steam does not exclusively react with gaseous species, but it also tends to interact with CaO in the acceptor material. The effect of the affinity of CaO to steam on SESRM has been reported evident in the initial stage of the SESRM reaction, referred as the induction period. Hildenbrand et al. have reported that there existed induction period of SESRM at S/C = 2–4, pressure = 1 atm, and temperature = 580 °C.<sup>31</sup> In another report, the apparent induction period could

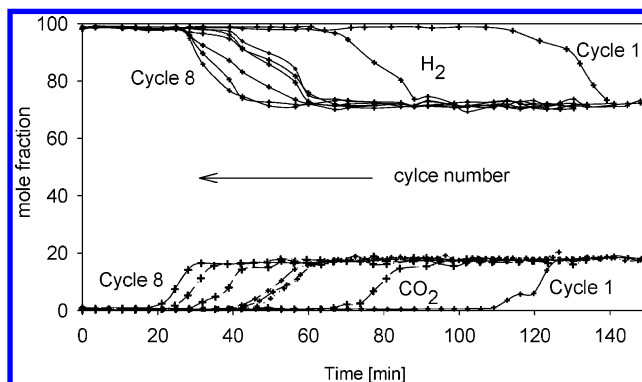


**Figure 6.** The evolution of H<sub>2</sub> and CO<sub>2</sub> contents in the 8 repeated cycles for the sorption enhanced steam reforming of ethanol. The conditions are the following: a temperature of 575 °C, a pressure of 1 atm, a steam-to-fuel ratio of 6, and a mixture of dolomite (10 g) and 30Co–10Ni/HTIs (2 g).

be found at the temperature <650 °C.<sup>32</sup> Such a high-temperature limit for the induction period is seemingly not consistent with the prediction by thermodynamics mentioned in the previous subsection. However, the thermodynamic analysis, based on the bulk material properties, does not answer surface-related questions. The affinity of CaO to steam permits H<sub>2</sub>O molecules to accumulate on the surface of CaO before the H<sub>2</sub>O molecules are involved into the steam reforming reaction on the surface of the catalyst. Such transit occupation of the H<sub>2</sub>O molecules has been speculated to decrease the availability of the steam to the steam reforming reaction in the start-up stage of the SESRM reaction.<sup>31,33</sup> As a result, low steam reforming efficiency has been observed during the induction period, indicated by high CH<sub>4</sub> content and low hydrogen content in the gas effluent.<sup>31,33</sup> After a certain time on stream, the population of the H<sub>2</sub>O molecules on the CaO surface reached the steady state. This allowed an increase of the actual S/C ratio in the steam reforming reaction, leading to improved methane conversion and hydrogen content in the gas effluent.

The above-mentioned induction period has been reported for the SESRM reaction. Interestingly, such induction period was nearly negligible in our study at the operating conditions similar to those reported for SESRM.<sup>31,33</sup> Obviously the induction period depends on the different fuels in SESR processes. There are parallel reactions on CaO surface leading to CaCO<sub>3</sub> and Ca(OH)<sub>2</sub>, respectively. The high reforming rate of ethanol and thus high rate for CO<sub>2</sub> generation might enhance the CaCO<sub>3</sub> formation. The short time period from the start-up to steady-state running of the SESRE reaction is advantageous in simplifying process operation and improving its applicability.

**C. Acceptor Performance.** The competitive features of the SESRE process largely rely on the properties of the acceptor in use. The main problem associated with CO<sub>2</sub> acceptors is the decay in their performance during many carbonation/decarbonation cycles. To study the dynamic properties of calcined dolomite sample and their effects on H<sub>2</sub> production in the SESRE process, the sessions of the carbonation/decarbonation (corresponding to the SESRE/regeneration) were repeated in 8 cycles. Results from such experiments are shown in Figure 6. Since the CO and CH<sub>4</sub> concentrations varied similarly with CO<sub>2</sub>, only the H<sub>2</sub> and CO<sub>2</sub> concentrations are plotted as a function of time and cyclic number.

The combined kinetic effect of the catalytic and CO<sub>2</sub> capture reaction is an important factor to the product distribution of the SESR reaction.<sup>34</sup> During the postbreakthrough stages, the contents of H<sub>2</sub> and CO<sub>2</sub> appeared at similar levels in the various

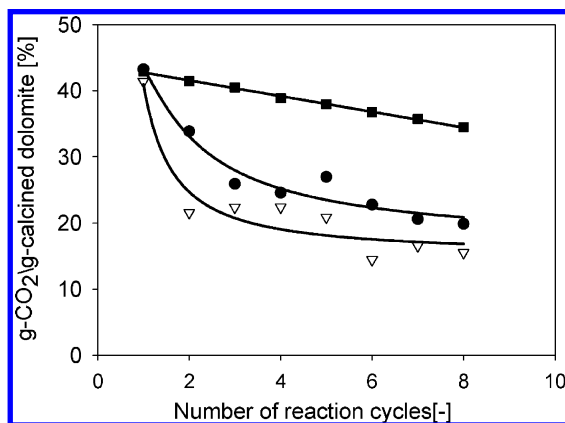


**Figure 7.** CO<sub>2</sub> capture capacity of calcined dolomite through 8 carbonation/decarbonation cycles assessed by means of TGA (■), TEOM (●) and in situ capture in the ethanol steam reforming process (▼). In the case of TGA, decarbonation at 700 °C and carbonation at 595 °C in 10% CO<sub>2</sub>/Ar; in the case of TEOM, decarbonation at 700 °C and carbonation at 595 °C in 10% CO<sub>2</sub>/40% H<sub>2</sub>O/Ar; in the case of in situ capture, decarbonation at 770 °C and carbonation at 575 °C in the gas mixture from steam reforming of ethanol.

cycles. Likewise, the levels of CO and CH<sub>4</sub> concentration after breakthrough showed negligible variation with the cyclic number. The repeated levels of the gas contents in the postbreakthrough stages of the various cycles might indicate that the catalytic reforming reactions behaved similarly in each cycle or there was no substantial change in the catalytic kinetics of steam reforming reactions. In the studied case, it allows us to assume that the stable catalytic reactions over cyclic operation could not be responsible for the cyclic variation in the evolution of the gas composition before the postbreakthrough stage took place. The cyclic variation might be associated along with the deterioration of CO<sub>2</sub> uptake, which can be classified into two cases, the loss of capture kinetics or capacity. It has been reported that, along with the decrease of the maximum capacity, the CO<sub>2</sub> capture kinetics of dolomite essentially decreases with the cyclic number.<sup>27,35</sup> Nevertheless, as seen in Figure 6, similar levels of H<sub>2</sub> and CO<sub>2</sub> content were repeated by the SESRE reaction or in the prebreakthrough stage of the various cycles. In addition, in each cycle there was no evident change in the time period of the breakthrough or the sharpness of the breakthrough curve, which has been correlated to the kinetics of the solid–gas reaction.<sup>36</sup> Accordingly, it is reasonable to say that the decay of the capture kinetics did not appear evident in the cyclic carbonation/decarbonation reaction. It might be explained by that the decay of the capture kinetics was slow in the sequential cycles and, consequently, the product gas composition of the SESRE reaction in each cycle was not influenced evidently. In fact, a similar conclusion with dolomite was also made on the SESRM reaction.<sup>10</sup>

Compared to the undetected decay in kinetics, the loss of maximum capacity was clearly demonstrated in the test. In Figure 6, the breakthrough proceeded earlier in the subsequent cycles. The decrease in the time period of the prebreakthrough is linked to the degradation of the capture capacity. As shown in Figure 6, the effective working period decreased from 110 min in the first cycle to 20 min in the eighth cycle.

The evolution of the capture capacity in the steam reforming atmosphere is compared with that assessed by TGA measurement in dry CO<sub>2</sub>/inert gas. The amount of CO<sub>2</sub> captured in the SESRE test was estimated by eq 11 and plotted in Figure 7. Different degradation trends were found in two tests. The CO<sub>2</sub> capture capacity decreased dramatically in the SESRE test in

the first two cycles with a loss of nearly half of initial capacity and then tended to decay slowly. In contrast, although the calcined dolomite sample in the first cycle of the TGA test displayed a similar capacity to that from the SESRE test, it had much better capacity and showed much slower degradation of activity in the following cycles of the TGA test under dry conditions. The comparatively high temperature of decarbonation in the SESRE process might be suspected to cause fast decline of the calcined dolomite. However, much harsh conditions (850 °C for carbonation and decarbonation) were applied in another independent test and only mild decrease in the capacity was observed.<sup>37</sup> A better explanation is needed for fast degradation in the SESRE process.

Indeed, there have been discussions on the capacity degradation of CaO-based acceptors after working in a mixture of steam and syn-gas.<sup>38,39</sup> Carbon formation is often observed in reforming processes and the subsequent buildup of coke on the acceptor surface is reported to have adverse effect on its performance. Even though the cyclic test was performed in a thermodynamically carbon-free operation regime, there was still doubt about coke formation since it is a typical kinetically controlled process. The TPO of spent catalyst or bed material is a common technique to assess coke formation from gasification or steam reforming process. However, the spent bed material from the SESRE process is a mixture of catalyst and CO<sub>2</sub> acceptor. CO<sub>2</sub> carbonation or decarbonation likely occurs at same temperature zone for burning the coke in air flow, typically used for the TPO measurement. To avoid interference of the carbonation/decarbonation reaction, TPO procedure was designed as the following. First, the CaO in the spent mixture of the catalyst and acceptor was saturated in a CO<sub>2</sub>-rich atmosphere. At elevated temperatures, air together with CO<sub>2</sub> was introduced to facilitate the oxidation of coke. According to eq 12, the chosen CO<sub>2</sub> partial pressure was high enough to prevent the decarbonation of the acceptor.<sup>40</sup> Therefore, the weight loss of the spent solid material in CO<sub>2</sub>/air atmosphere can be attributed to burning of coke. Our measurement on the selected mixture discovered no appreciable amount of coke deposited. It leads to a conclusion that coke deposition might not be a main reason to the fast degradation of the CO<sub>2</sub> uptake capacity.

$$K_a = P_{\text{CO}_2}^{\text{eq}} = \exp(\Delta G_{\text{rxn}}^{\circ}(T)/RT) \quad (12)$$

The degradation in the uptake capacity of the acceptor is often caused by sintering, which is mainly controlled by the property of the acceptor material, operating temperature, and atmosphere.<sup>41</sup> Considering that all the mentioned TGA experiments were conducted under dry conditions, a cyclic test in the presence of steam was performed by using TEOM. The obtained results were plotted in Figure 7, together with those from the TGA and SESRE test. The deactivation tendency shown in the TEOM test is comparable to that presented in the SESRE test. It leads to assumption that the rapid degradation of the dolomite might be a result of accelerated sintering by steam. Sintering can cause the prompt closure of the pores throughout the particles and reduce the surface area of the CaO particles.<sup>41</sup> As a result, it hampers the carbonation reaction by inhibiting CO<sub>2</sub> accessible to the unreacted CaO. The acceptor material with formation of CaCO<sub>3</sub> has low resistance to sintering since CaCO<sub>3</sub> has a melting point at 1339 °C, considerably lower than 2927 °C for CaO. CaCO<sub>3</sub> is prone to fast sintering in the presence of steam, compared with under dry conditions.<sup>42,43</sup> The catalytic effect of steam is particularly evident at high temperatures relevant to the SESRE operation.

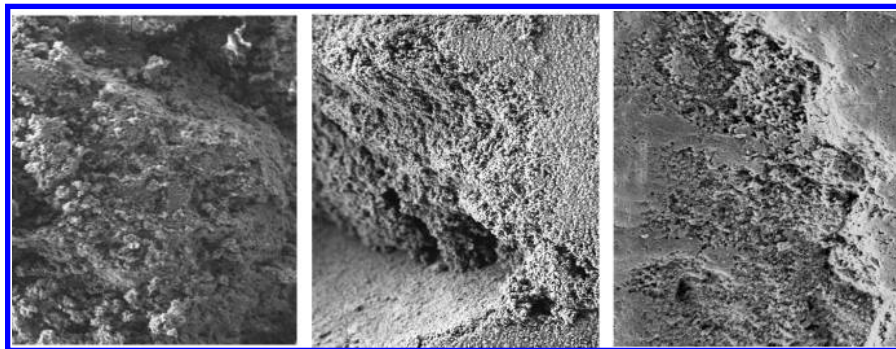


**Figure 8.** SEM images (magnification 5000 $\times$ ) for fresh calcined (left), after dry carbonation cycles on TGA (middle), and 8 cycles for the sorption enhanced steam reforming of ethanol (right).

On the basis of the above discussion there appears to be merit in investigating the morphology of the calcined dolomite since solid particles typically tend to aggregate closely during the course of sintering. In Figure 8, SEM images illustrate morphological variations on the dolomite samples treated in different atmospheres. The fresh calcined dolomite appeared as a porous and rough texture. After cycles of the carbonation/decarbonation in the dry condition, the pores tended to diminish. More compact small particles were formed due to the breaking up of the particles. It has been reported that the dolomite sample after 11 cycles of carbonation-decarbonation gave higher surface area than the fresh calcined sample.<sup>44</sup> This has been accounted for by the presence of smaller particles. After subjected to repeated cycles of the SESRE process, the surface of the dolomite became smoother and large pores were formed. Sintering bridges and fusing of particles were observed, indicating that severe agglomeration and sintering occurred on the dolomite.

#### IV. Conclusions

The chemical equilibrium analysis has been carried out to compare the conventional and CaO–CO<sub>2</sub> capture coupled steam reforming of ethanol. H<sub>2</sub> output can be considerably enhanced by coupling CO<sub>2</sub> removal in the steam reforming process. Very pure H<sub>2</sub> can be produced via the SESRE reaction, operated at temperatures from 500 to 600 °C and S/C > 3. Low pressure favors H<sub>2</sub> production by eliminating hydration of CaO and promoting steam reforming reactions. At high pressures, H<sub>2</sub> purity can still be twice as high as the conventional steam reforming. By choosing suitable conditions for the SESRE reaction, it is possible to incorporate three processes typical for fuel reforming (steam reforming, CO and CO<sub>2</sub> removal) in one single reactor. In addition, low risk of carbon formation is expected due to that the addition of CO<sub>2</sub> acceptor shifts carbon formation boundary to low S/C regimes.

The new sorption-assisted reaction process was examined by using a series of Co–Ni/HTIs catalysts and calcined dolomite as CO<sub>2</sub> acceptor. The obtained highest H<sub>2</sub> purity of more than 99% was realized over the 40Ni and 20Co–20Ni/HTIs catalyst at a temperature of 550 °C. Such H<sub>2</sub> content in the product gas was fairly close to the equilibrium value, suggesting a fine match between catalytic activity and CO<sub>2</sub> capture in the chosen reaction conditions. At such optimal operating temperature, the H<sub>2</sub> purity was limited mainly by the thermodynamic boundary of CO<sub>2</sub> partial pressure. In other cases, product gas composition was governed by the kinetic limits imposed by the CO<sub>2</sub> capture or catalytic reactions. In the high-temperature regime, the main impurity in H<sub>2</sub> production was CO<sub>2</sub> as well as CO while CH<sub>4</sub> was dominant byproduct at the low temperatures. Interestingly, unlike the results from SESRM, no long induction period was

observed in the SESRE reaction process. It suggests that the steam interaction with CaO in the acceptor had weak influence on the enhancement of H<sub>2</sub> production at the initial stage of the SESRE reaction. In addition, the cyclic stability in CO<sub>2</sub> capture of the calcined dolomite was examined by repeating the SESRE reaction. The decay in the kinetics of CO<sub>2</sub> capture did not evidently have influence on the SESRE reaction while the fast decrease in the maximum capacity of dolomite was observed in the consecutive cycles. By comparing the results from the independent cyclic tests under wet and dry conditions, the fast deactivation of the acceptor was attributed to the catalytic effect of the steam on the sintering of the acceptor material. It was further confirmed with the SEM images, in which the spent dolomite after multicycle operation of SESRE appeared a great degree of sintering.

The attractiveness of SESRE reaction process has been proved for H<sub>2</sub> production. Today, the main problem associated with the application of the new reaction process is deactivation of the acceptor in multicyclic operation. This problem may be solved by developing new synthetic acceptor with improved stability.

**Acknowledgment.** The financial support by the Research Council of Norway (NFR) through the CLIMIT program is gratefully acknowledged. Dr. Tiejun Zhao, Dept. of Chem. Eng. NTNU, is acknowledged for conducting the TEOM experiment.

#### References and Notes

- (1) Kikuchi, R.; Gerardo, R.; Santos, S. M. *Int. J. Energy Res.* **2009**, *33*, 186.
- (2) Haryanto, A.; Fernando, S.; Murali, N.; Adhikari, S. *Energy Fuels* **2005**, *19*, 2098.
- (3) Ni, M.; Leung, D. Y. C.; Leung, M. K. H. *Int. J. Hydrogen Energy* **2007**, *32*, 3238.
- (4) Benito, M.; Sanz, J. L.; Isabel, R.; Padilla, R.; Arjona, R.; Daza, L. *J. Power Sources* **2005**, *151*, 11.
- (5) Vaidya, P. D.; Rodrigues, A. E. *Chem. Eng. J.* **2006**, *117*, 39.
- (6) Barelli, L.; Bidini, G.; Gallorini, F.; Servili, S. *Energy* **2008**, *33*, 554.
- (7) Batista, M. S.; Assaf, E. M.; Assaf, J. M.; Ticianelli, E. A. *Int. J. Hydrogen Energy* **2006**, *31*, 1204.
- (8) Harrison, D. P. *Ind. Eng. Chem. Res.* **2008**, *47*, 6486.
- (9) Yoon, Y. I.; Baek, I. H.; Park, S. D. *J. Ind. Eng. Chem.* **2007**, *13*, 842.
- (10) Johnsen, K.; Ryu, H. J.; Grace, J. R.; Lim, C. J. *Chem. Eng. Sci.* **2006**, *61*, 1195.
- (11) Lee, K. B.; Beaver, M. G.; Caram, H. S.; Sircar, S. *Ind. Eng. Chem. Res.* **2007**, *46*, 5003.
- (12) Harrison, D. P. *Energy Procedia* **2009**, *1*, 675.
- (13) Lysikov, A. I.; Trukhan, S. N.; Okunev, A. G. *Int. J. Hydrogen Energy* **2008**, *33*, 3061.
- (14) Iwasaki, Y.; Suzuki, Y.; Kitajima, T.; Sakurai, M.; Kameyama, H. *J. Chem. Eng. Jpn.* **2007**, *40*, 178.
- (15) Essaki, K.; Muramatsu, T.; Kato, M. *Int. J. Hydrogen Energy* **2008**, *33*, 6612.



- (16) Ochoa-Fernandez, E.; Haugen, G.; Zhao, T.; Ronning, M.; Aartun, I.; Borresen, B.; Rytter, E.; Ronnekleiv, M.; Chen, D. *Green Chem.* **2007**, *9*, 654.
- (17) Kuramoto, K.; Fujimoto, S.; Morita, A.; Shibano, S.; Suzuki, Y.; Hatano, H.; Lin, S. Y.; Harada, M.; Takarada, T. *Ind. Eng. Chem. Res.* **2003**, *42*, 975.
- (18) Silaban, A.; Narcida, M.; Harrison, D. P. *Chem. Eng. Commun.* **1996**, *146*, 149.
- (19) He, L.; Berntsen, H.; Ochoa-Fernandez, E.; Walmsley, J. C.; Blekkan, E. A.; Chen, D. *Top. Catal.* **2009**, *52*, 206.
- (20) Chen, D.; Bjorgum, E.; Christensen, K. O.; Holmen, A.; Lodeng, R. *Adv. Catal.* **2007**, *51*, 351.
- (21) Ochoa-Fernandez, E.; Zhao, T. J.; Ronning, M.; Chen, D. *J. Environ. Eng., ASCE* **2009**, *135*, 397.
- (22) Prins, M. J.; Ptasiński, K. J.; Janssen, F. J. J. G. *Chem. Eng. Sci.* **2003**, *58*, 1003.
- (23) Vagia, E. C.; Lemonidou, A. A. *Int. J. Hydrogen Energy* **2007**, *32*, 212.
- (24) Wang, H.; Wang, X.; Li, M.; Li, S.; Wang, S.; Ma, X. *Int. J. Hydrogen Energy* **2009**, *34*, 5683.
- (25) Rossi, C. C. R. S.; Alonso, C. G.; Antunes, O. A. C.; Guirardello, R.; Cardozo-Filho, L. *Int. J. Hydrogen Energy* **2009**, *34*, 323.
- (26) Luo, N.; Zhao, X.; Cao, F.; Xiao, T.; Fang, D. *Energy Fuels* **2007**, *21*, 3505.
- (27) Alonso, M.; Rodríguez, N.; Grasa, G.; Abanades, J. C. *Chem. Eng. Sci.* **2009**, *64*, 883.
- (28) Bhatia, S. K.; Perlmutter, D. D. *AIChE J.* **1983**, *29*, 79.
- (29) Dedman, A. J.; Owen, A. J. *Trans. Faraday Soc.* **1962**, *58*, 2027.
- (30) Mess, D.; Sarofim, A. F.; Longwell, J. P. *Energy Fuels* **1999**, *13*, 999.
- (31) Vaidya, P. D.; Rodrigues, A. E. *Chem. Eng. J.* **2006**, *117*, 39.
- (32) Hildenbrand, N.; Readman, J.; Dahl, I. M.; Blom, R. *Appl. Catal., A* **2006**, *303*, 131.
- (33) Lin, S.; Harada, M.; Suzuki, Y.; Hatano, H. *Fuel* **2002**, *81*, 2079.
- (34) Balasubramanian, B.; Lopez Ortiz, A.; Kaytakoglu, S.; Harrison, D. P. *Chem. Eng. Sci.* **1999**, *54*, 3543.
- (35) Rusten, H. K.; Ochoa-Fernandez, E.; Chen, D.; Jakobsen, H. A. *Ind. Eng. Chem. Res.* **2007**, *46*, 4435.
- (36) Li, Q. Z.; Zhou, W.; Chen, H. C. *Fuel Process. Technol.* **2008**, *89*, 1461.
- (37) Dou, B.; Chen, B.; Gao, J.; Sha, X. *Energy Fuels* **2005**, *19*, 2229.
- (38) Sun, P.; Grace, J. R.; Lim, C. J.; Anthony, E. J. *Energy Fuels* **2007**, *21*, 163.
- (39) Corella, J.; Toledo, J. M.; Molina, G. *Ind. Eng. Chem. Res.* **2006**, *45*, 6137.
- (40) Delgado, J.; Aznar, M. P.; Corella, J. *Ind. Eng. Chem. Res.* **1996**, *35*, 3637.
- (41) Sandler, S. I. *Chemical and engineering thermodynamics*, 3rd ed.; Wiley: New York, 1999.
- (42) Borgwardt, R. H. *Ind. Eng. Chem. Res.* **1989**, *28*, 493.
- (43) L'vov, B. V. *Thermochim. Acta* **1997**, *303*, 161.
- (44) Readman, J. E.; Blom, R. *Phys. Chem. Chem. Phys.* **2005**, *7*, 1214.

JP906146Y